Ferroelectric phase transitions of 3*d*-spin origin in $Eu_{1-x}Y_xMnO_3$

Y. Yamasaki,[1] S. Miyasaka,[1,*] T. Goto,[1] H. Sagayama,[2] T. Arima,[2,3] and Y. Tokura[1,3,4]
[1]*Department of Applied Physics, University of Tokyo, Tokyo 113-8656, Japan*
[2]*Institute of Multidisciplinary Research for Advanced Materials, Tohoku University, Sendai 980-8577, Japan*
[3]*Spin Superstructure Project and Multiferroics Project, ERATO, Japan Science and Technology Agency, Tsukuba 305-8562, Japan*
[4]*Correlated Electron Research Center (CERC), National Institute of Advanced Industrial Science and Technology (AIST), Tsukuba 305-8562, Japan*
(Received 18 June 2007; published 15 November 2007)

Perovskite-type rare-earth manganites RMnO$_3$ (R=Tb and Dy) undergo the ferroelectric transitions concomitantly with the collinear to noncollinear magnetic transitions of Mn 3*d* spins, in which the electric polarization direction can be controlled by an external magnetic field. To clarify how the magnetic transition of Mn 3*d* spins is correlated with the ferroelectric transition, we have investigated a mixed-crystal system of perovskite-type $Eu_{1-x}Y_xMnO_3$ ($0 \leqslant x \leqslant 0.4$) without the 4*f* magnetic moments of the rare earth ions. The choice of the present system has enabled us to systematically investigate the correlation between dielectric, magnetic (of Mn spin origin), and superlattice properties with varying the perovskite lattice distortion or equivalently the competing Mn spin superexchange interactions. The compounds with x=0.3 and 0.4 undergo the ferroelectric transitions with the spontaneous polarization along the *a* axis, which is associated with the formation of a *ab*-plane cycloidal spin structure with the modulation vector along the *b* axis. Among them, the x=0.4 compound was found to undergo the polarization flop from along the *a* axis to the *c* axis as induced not only thermally but also by a magnetic field applied along the *a* axis. The magnetic-field induced polarization flop and its mechanism for x=0.4 can be fully accounted for in terms of the rotation of the cycloidal spin plane from *ab* to *bc* stemming from the Mn spin flops. This is contrasted by the case of TbMnO$_3$ and DyMnO$_3$ with the rare-earth 4*f* Ising moments coupled to the Mn 3*d* spins, in which magnetic fields along the *b* axis and the *a* axis, but not along the *c* axis (up to 14 T), can flop the polarization from along the *c* axis to the *a* axis.

DOI: 10.1103/PhysRevB.76.184418 PACS number(s): 75.80.+q, 78.70.Ck

I. INTRODUCTION

Magnetic control of electric polarization in magnetic ferroelectrics, in which (anti)ferromagnetism and ferroelectricity order coexist, have recently been investigated extensively. Mutual control of dielectric and magnetic properties has been known as the magnetoelectric (ME) effect and has long been attracting appreciable interest from both fundamental and practical points of view, yet its magnitude has remained too small for actual application.[1] The problem is how to design such a multiferroic material and how to enhance its ME coupling.[2] A useful hint for designing the strong ME coupling has been obtained by the discovery of ferroelectricity in cycloidal-spin magnets, perovskite-type rare-earth manganites RMnO$_3$ (R=Tb and Dy).[3–5]

Orthorhombically distorted perovskite-type rare-earth manganites TbMnO$_3$ and DyMnO$_3$ show strong interplay between magnetic and dielectric properties. According to recent neutron diffraction measurements, the ferroelectric polarization emerges in accord with Mn 3*d* spin collinear to noncollinear (elliptically cycloidal) magnetic transition.[6–8] For example, TbMnO$_3$ undergoes the successive transitions to the incommensurate spin order with lowering temperature, at first to the collinear sinusoidal state at T_N=42 K and then to the transverse-spiral or cycloidal state at T_C=27 K. Upon the latter collinear to cycloidal spin transition at T_C, the ferroelectric state is observed to emerge, irrespective of the spin modulation being commensurate or incommensurate.[6,8] In fact, $Tb_{0.32}Dy_{0.68}MnO_3$ undergoes the transition to the commensurate spin order with wave vector $\boldsymbol{Q}_m$=(01/31) immediately below T_N (~40 K) and then to the ferroelectric phase transition at T_C (~20 K) without changing the wave vector but with the collinear to cycloidal spin transition.[7] Therefore, the ferroelectric transition is certainly induced by the Mn 3*d* spins collinear to noncollinear transition rather than incommensurate-commensurate or lock-in transition in RMnO$_3$.

The direction of the spontaneous polarization is perpendicular to the propagation vector in the ferroelectric phase of RMnO$_3$. The feature is in accord with the antisymmetric exchange mechanism (inverse Dzyaloshinskii-Moriya interaction)[9–11] for the magnetic ferroelectricity. When the cycloidal or transverse-spiral spin order is realized, the uniform spontaneous polarization is expected to be present in the direction perpendicular to the cycloidal propagation vector $\boldsymbol{Q}_m$ and spin rotation axis. The models lead to the relation between the polarization ($\boldsymbol{P}_{ij}$) and the spin vector chirality ($\boldsymbol{C}_{ij}=\boldsymbol{S}_i \times \boldsymbol{S}_j$) for the neighboring two sites (i and j), $\boldsymbol{P}_{ij}=A\boldsymbol{e}_{ij} \times \boldsymbol{C}_{ij}$. Here, $\boldsymbol{e}_{ij}$ denotes the vector connecting the two sites, and A is the proportional constant as determined by the spin exchange interaction and spin-orbit interaction.[11] This is the origin of the magnetic ferroelectricity observed not only for RMnO$_3$ but also for other magnetic ferroelectrics, such as the cycloidal type of $Ni_3V_2O_8$,[12] $MnWO_4$,[13] $LiCu_2O_2$,[14] and the transverse cone-spiral type of $CoCr_2O_4$.[15]

The remarkable ME effects have been demonstrated for RMnO$_3$ (R=Tb and Dy) with such magnetic ferroelectricity. The spontaneous polarization along the *c* axis $P \| c$ (P_c) is flopped to the *a* axis $P \| a$ (P_a) by applying a magnetic field along the *b* axis $H \| b$ (H_b).[3–5] In spite of extensive investi-

gations on the mechanism of such a polarization rotation, the conclusive assignment has not been obtained as yet.[16,17] A possible mechanism of the polarization flop has been proposed by Mostovoy:[9] In the ferroelectric phase with spiral spin ordering, the strong magnetic field will force the spiral basal plane to rotate to the perpendicular direction to the initial plane, leading to the flop of the direction of electric polarization. In the case of a cycloidal magnet with the spin spiral plane on the *bc* plane, application of magnetic field along the *b* axis (H_b) or the *c* axis (H_c) would induce the flop of the spiral plane from *bc* to *ac* or to *ab*, respectively, if the magnetic anisotropy of spins were not effective. However, the case of the magnetic field effect observed in $TbMnO_3$ shows the discrepancy from this conjecture; the change of the spin spiral plane is from *bc* to *ab* plane by applying H_b or H_a, but not H_c. It was also argued[9] that this unusual behavior is related to the flop of the Ising-like rare earth 4*f* moments coupled Mn 3*d* spins, and that the additional higher-order anisotropies are needed to explain the mechanism of electric polarization flop in rare-earth manganites.

In this context, one of the important issues that remain to be clarified in relevance to the magnetic control of electric polarizations in rare-earth manganites is the change and its mechanism of Mn 3*d* spin structure induced thermally and/or by external magnetic field. It has been reported that the ferroelectric transition and polarization flop by applying magnetic field are also observed in a mixed-crystal system $Eu_{1-x}Y_xMnO_3$ with comparable lattice distortions (tolerance factor) to $TbMnO_3$.[18,19] We have investigated comprehensively the lattice-structural, magnetic, and ferroelectric properties of single crystalline $Eu_{1-x}Y_xMnO_3$ ($0 \leqslant x \leqslant 0.4$). We present a synchrotron radiation x-ray diffraction study of $Eu_{1-x}Y_xMnO_3$ to measure the lattice modulation vector, which is closely tied to the magnetic modulation vector. Therefore, the nature of change in Mn 3*d* spin structure along with the ferroelectric transitions can be derived from the change of lattice modulation by a synchrotron x-ray measurement. The choice of this mixed-crystal system enables us to systematically investigate the magnetic anisotropy of Mn spin origin as well as the magnetoelectric phase diagram with changing the orthorhombic lattice distortion governing the frustrated spin exchange interactions, while eradicating the influence of the 4*f*-moment on the Mn 3*d* spins because of no magnetic moment for $Eu^{3+}(4f^6)$ and $Y^{3+}(4f^0)$.

II. EXPERIMENTS

Polycrystals of $Eu_{1-x}Y_xMnO_3$ ($0 \leqslant x \leqslant 0.4$) were first prepared by a conventional solid-state reaction. The orthorhombically distorted perovskite structure (space group *Pbnm* at room temperature) without any trace of impurity phase was confirmed to be present in the atmospheric pressure synthesis up to $x=0.4$, while a minute amount of hexagonal phase was discerned around $x=0.45$ and no pure perovskite-type phase above $x=0.45$. Single crystals of $Eu_{1-x}Y_xMnO_3$ ($x=0-0.4$) were grown by the floating zone method at a feed rate of 6 mm/h in an Ar atmosphere. The crystals were oriented using Laue XRD pattern, and cut into thin plates with the widest faces perpendicular to the crystallographic principal axes. Silver paste was painted at the end surfaces as the electrodes. The temperature and magnetic field dependence of the electric polarization *P* was obtained by measurements of pyroelectric (or displacement) current with applying electric field (200 kV/m). The dielectric constant was measured with an LCR meter at a frequency of 10 kHz. Magnetization measured with a dc magnetometer up to 9 T. The superlattice structure associated with the commensurate or incommensurate magnetic order was searched for along the (0 *k* 1) direction in the reciprocal space in terms of synchrotron-radiation x-ray diffraction. Nonresonant single-crystal x-ray diffraction was measured on the Beamlines 4C and 16A1, Photon Factory of KEK. X-ray was monochromatized to 16 keV for the Beamline 4C and to 13 keV for 16A1 with Si(111) double crystal and focused on the sample in a cryostat equipped with a superconducting magnet. Superlattice diffractions were measured in magnetic fields applied parallel to the *a* axis $H \| a$ (H_a) up to 8 T on the Beamline 16A1.

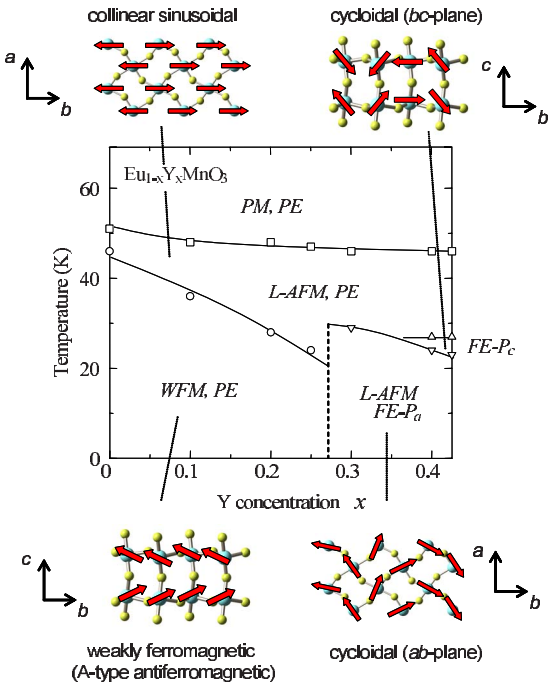

FIG. 1. (Color online) Magnetic and dielectric phase diagram of $Eu_{1-x}Y_xMnO_3$ as a function of Y concentration *x* in the absence of magnetic field. Schematic magnetic structures are shown for the respective magnetic phases. Open squares, circles and triangles denote the transition temperatures of the paramagnetic (PM) to long-wavelength antiferromagnetic (LAFM) phase, the LAFM to weakly ferromagnetic phase (WFM), and the paraelectric (PE) to ferroelectric phase with the electric polarization along the *a* axis (FE-P_a) or *c* axis (FE-P_c), respectively. Solid and dashed lines are merely the guide to the eyes.

III. RESULTS

Figure 1 shows the magnetoelectric (*x*-*T*) phase diagram as function of yttrium concentration *x* in the absence of magnetic field for our single crystals of $Eu_{1-x}Y_xMnO_3$. For all the compounds with $0 \leqslant x \leqslant 0.4$, the long-wavelength antifer-

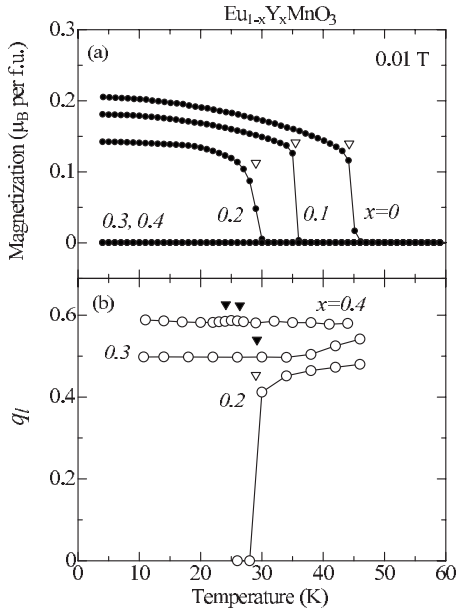

FIG. 2. The temperature dependence of (a) magnetization along the c axis (M_c) and (b) wave number q_l of lattice modulation (or equivalently $q_m=\frac{1}{2}q_l$ of magnetic modulation) along the b axis in $Eu_{1-x}Y_xMnO_3$ with various x. The closed and open triangles indicate the ferroelectric transition and the weakly ferromagnetic one, respectively.

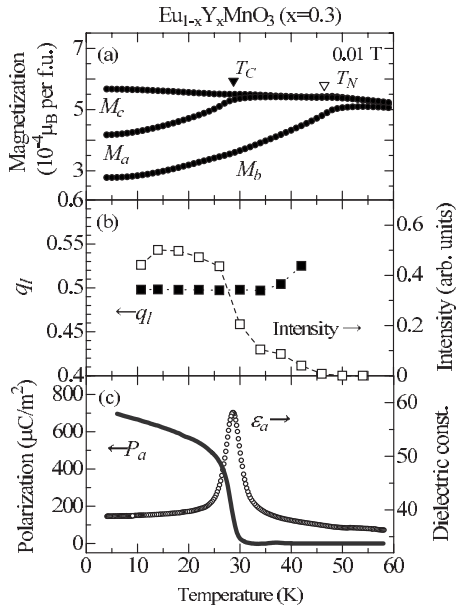

FIG. 3. Temperature dependence of (a) magnetization for each crystal axis, (b) lattice modulation vector q_l and integrated intensity of the $(0\ 4-q_l\ 1)$ superlattice reflection, and (c) dielectric constant ε_a and electric polarization P_a measured along the a axis in $Eu_{0.7}Y_{0.3}MnO_3$. The closed and open triangles indicate the temperatures of the Mn spin collinear order (T_N) and the ferroelectric transition (T_c), respectively.

romagnetic (LAFM) phases appear below the magnetic ordering temperature (T_N). At the lowest temperature, there appears a weakly ferromagnetic phase (WFM) with the spontaneous magnetization along the c axis $M\|c(M_c)$ in the low-x region of $0\leqslant x\leqslant 0.2$, and two ferroelectric phases with the electric polarization along the a axis (FE-P_a) and the c axis (FE-P_c) in the region of $0.3\leqslant x$. The essentially identical magnetic and dielectric phase diagrams have recently been reported for this $Eu_{1-x}Y_xMnO_3$ system independently by two research groups.[18–21] We show in Figs. 2(a) and 2(b) the temperature dependence of magnetization along the c axis (M_c) under a weak magnetic field of 0.01 T for $0\leqslant x\leqslant 0.4$ and of the lattice modulation wave number (q_l) for $0.2\leqslant x\leqslant 0.4$, respectively. The satellite reflection with lattice modulation vector $\boldsymbol{Q}_l=(0\ q_l\ 0)$ as observed for the LAFM phase arises from the exchange-striction type spin-lattice interaction; the Mn spin moments with a modulation vector $\boldsymbol{Q}_m=(0\ q_m\ 1)$ cause the lattice modulation with $q_l=2q_m$ in $RMnO_3$.[3,16] For $x=0.2$, the superlattice reflections observed in the LAFM phase disappear upon the phase transition to the WFM phase with lowering temperature, as shown in Fig. 2. In the WFM phase, the Mn 3d spins are aligned ferromagnetically in the ab-plane without spin modulation ($q_m=0$) and coupled antiferromagnetically along the c-axis where the weak spontaneous magnetization appears along the c-axis (M_c) due to the Dzyaloshinskii-Moriya interaction.[22,23] The substitution of Eu^{3+} with Y^{3+} decreases the average Mn-O-Mn bond angle and tends to enhance the antiferromagnetic interaction between the next-nearest-neighbor Mn ions in the ab plane and hence the magnetic frustration.[24] With the increase of x, the onset temperature of the WFM phase decreases, while the LAFM phase subsists down to the lowest temperature [Fig. 2(b)].

In the region of $x\geqslant 0.3$, there are two ferroelectric phases (FE-P_a and FE-P_c) with spontaneous polarization along the a axis and c axis, respectively. In these ferroelectric phases, the magnetization shows a remarkable anisotropic behavior that is ensured to arise from the Mn spins by the advantage of using nonmagnetic A-site ions (Eu^{3+} and Y^{3+}). As shown in Fig. 3(a) for the $x=0.3$ compound, the magnetization along the b axis (M_b) steeply decreases at $T_N=46$ K, while the magnetization along the a axis (M_a) and c axis (M_c) remains unchanged. This suggests that Mn 3d spins are antiferromagnetically and collinearly aligned along the b axis, i.e., perpendicularly to the a and c axes. The onset temperature of the superlattice reflections is in accordance with the magnetic order as shown in Fig. 3(b). Therefore, in the temperature region of $29\ \text{K}<T<46$ K, Mn 3d spins should be sinusoidally and collinearly modulated along the b axis as observed for $TbMnO_3$ in the similar temperature region.[3,6,8] The present compound undergoes the ferroelectric phase transition with the spontaneous polarization along the a axis at 29 K [Fig. 3(c)], in contrast with the case of $TbMnO_3$ and $DyMnO_3$ where the thermally induced polarization is along the c axis. The magnetization along the a axis (M_a) decreases at the ferroelectric transition while M_c remains nearly constant. Such an anisotropic magnetization behavior indicates that Mn 3d spins lie in the ab plane in a noncollinear manner, such as spiral or elliptical magnetic structure as observed in the ferroelectric phase of $TbMnO_3$.[6–8] (Note, however, that the spin spiral plane for $TbMnO_3$ lies within the bc plane with the spontaneous polarization along the c axis.)

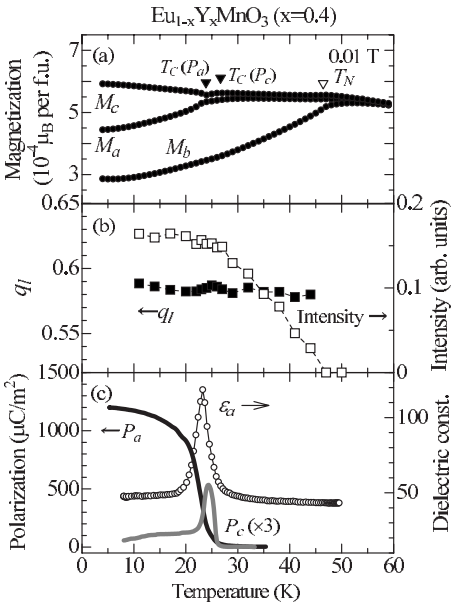

FIG. 4. Temperature dependence of (a) magnetization for each crystal axis, (b) lattice modulation wave number q_l and integrated intensity of the $(0\ 4-q_l\ 1)$ superlattice reflection, and (c) dielectric constant ε_a and electric polarization P_a (solid line) and P_c (gray line) in $Eu_{0.6}Y_{0.4}MnO_3$. The closed and open triangles indicate the temperature of Mn spin order (T_N) and the ferroelectric transition (T_c), respectively.

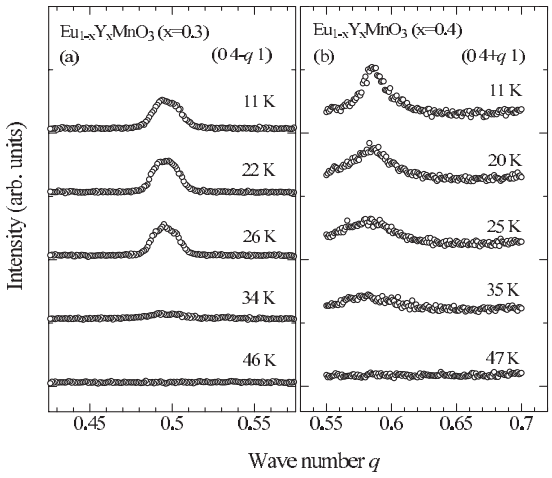

FIG. 5. Synchrotron x-ray diffraction profiles along (a) the $(0\ 4-q\ 1)$ line for $x=0.3$ and (b) the $(0\ 4+q\ 1)$ line for $x=0.4$ at selected temperatures. The respective profiles in (a) and (b) are displaced vertically for clarification.

As shown in Fig. 4, the ferroelectric transition associated with the similarly anisotropic magnetization behavior is also observed for $Eu_{0.6}Y_{0.4}MnO_3$ ($x=0.4$). This compound undergoes the successive transitions to the collinear sinusoidal state at 46 K, to the ferroelectric phase with the electric polarization along the c axis (FE-P_c) at $T_c(P_c)=26$ K, and then to the ferroelectric phase FE-P_a at $T_c(P_A)=24$ K [Fig. 4(c)]. Therefore, the spontaneous rotation of the ferroelectric polarization occurs with changing temperature even at zero magnetic field for $Eu_{0.6}Y_{0.4}MnO_3$, while for $TbMnO_3$ an external magnetic field (e.g., 5 T at 10 K) is needed for the rotation of polarization. Note that the M_c show a tiny drop at $T_c(P_c)$, but slightly increases again at $T_c(P_a)$. On the other hand, M_a begins to largely decrease from $T_c(P_A)$, but not from $T_c(P_c)$. These temperature-dependent variation of the anisotropic magnetic features again support the idea that P_a arise from the ab-plane spiral structure while P_c from the bc-plane spin spiral one, as supplemented also by the following discussions.

For both $x=0.3$ and 0.4 compounds that undergo the ferroelectric phase transition, lattice modulations arising from the spin superstructure are observed down to the lowest temperature (Fig. 5). The wave number for $x=0.3$ is commensurate as locked at $q_l=0.5$ below the ferroelectric phase transition temperature T_c. For $x=0.4$, by contrast, the lattice modulation q_l remains incommensurate and nearly constant $q_l\sim 0.58$ through T_c down to the lowest temperature. Electric polarization along the a axis in the commensurate phases ($q_l=0.5$) are also observed $TbMnO_3$ and $GdMnO_3$ when a magnetic field is applied along the b axis.[16] Two possible magnetic structures, the noncollinear spin structure such as the cycloidal spins rotating in the ab plane and the collinear spin structure, have been proposed for the origin of such a P_a phase.[16,17] Ferroelectric polarization can be explained by the antisymmetric exchange (inverse Dzyaloshinskii-Moriya interaction) model in the former noncollinear magnetic structure irrespective of the commensurate or incommensurate modulation, or otherwise by symmetric exchange striction (inverse Goodenough-Kanamori interaction) model in the latter but only for the commensurate modulation.[16,17,25] As for the present $Eu_{1-x}Y_xMnO_3$ series, since only the antisymmetric exchange model can explain an electric polarization in the incommensurate phase, the ferroelectric phase of $Eu_{0.6}Y_{0.4}MnO_3$ should show a noncollinear magnetic structure. Although the detail magnetic structure, collinear or cycloidal, for the P_a phase of $TbMnO_3$ and $GdMnO_3$ have not been determined, it is quite likely from the anisotropic magnetic properties commonly observed for $x=0.3$ [Fig. 3(a)] and $x=0.4$ [Fig. 4(a)] that the ferroelectric state of $Eu_{0.7}Y_{0.3}MnO_3$ with the commensurate order also takes the former noncollinear magnetic structure such as elliptical cycloid.

We have also investigated the effect of magnetic field H_a in the ferroelectric polarization. Figure 6(a) summarizes the results in terms of the magnetoelectric phase diagram (H-T diagrams) of $x=0.4$. The compound shows the magnetic field induced flop of the electric polarization between P_a and P_c, but the phase diagram differs considerably from those of $TbMnO_3$ [as depicted in Fig. 6(b)] and $DyMnO_3$. First, the direction of the driving magnetic field is parallel to a ($H\|a$) for $Eu_{1-x}Y_xMnO_3$ ($x=0.3-0.4$) and not to b ($H\|b$) nor c ($H\|c$) up to 14 T, while $H\|b$ (and $H\|a$, albeit higher H) for $TbMnO_3$ and $DyMnO_3$. Second, the critical magnetic field for the polarization flop increases with the decrease of temperature in $Eu_{0.6}Y_{0.4}MnO_3$, while with the increase of temperature in $TbMnO_3$ and $DyMnO_3$. (As for the reverse increase of the transition field below 10 K for $TbMnO_3$ [Fig. 6(b)], the first-order nature of the polarization flop transition

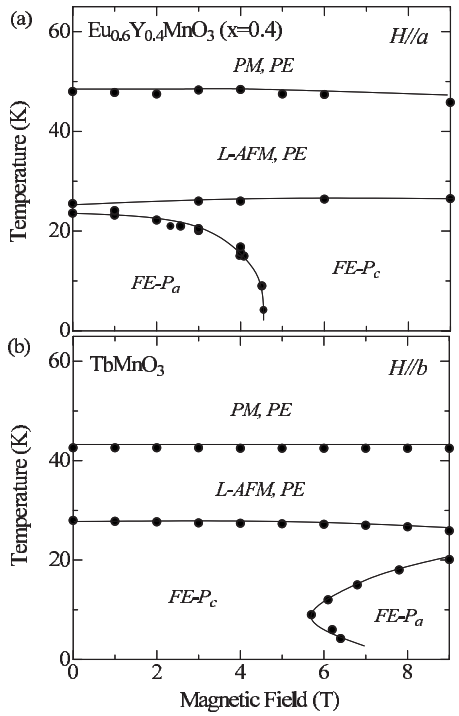

FIG. 6. Magnetoelectric phase diagram of (a) $Eu_{0.6}Y_{0.4}MnO_3$ for magnetic field applied along the *a* axis ($H \| a$) and (b) $TbMnO_3$ for magnetic field along the *b* axis ($H \| b$) (cited from Ref. 5).

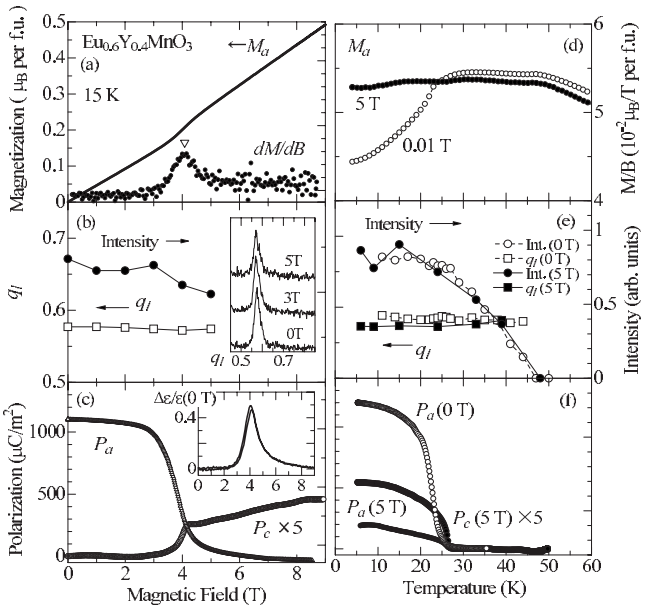

FIG. 7. Magnetic field and temperature dependences of magnetization (a), (d), lattice modulation wave number q_l (b), (e), and dielectric properties (c), (f) for magnetic field (H_a) applied along the *a* axis in $Eu_{0.6}Y_{0.4}MnO_3$. Inset to (b) shows the x-ray diffraction profiles along $(0,4-q,1)$ at various magnetic fields and to (c) shows the magnetic field (H_a) dependence of dielectric constant $[\Delta\epsilon_a/\epsilon_a(0\ \mathrm{T})]$.

causes the apparent supercooling effect in the field increasing run.[3,5]). Since the action of $4f$ moments of Tb^{3+} or Dy^{3+} is enhanced at lower temperatures, the polarization flop should be induced through $4f$-$3d$ interactions in $TbMnO_3$ and $DyMnO_3$, whereas the magnetic field acts directly on Mn $3d$ spin in the course of the polarization flop in $Eu_{0.6}Y_{0.4}MnO_3$.

Figure 7 shows the magnetic field and temperature dependence of the magnetization, lattice modulation wave number, and electric polarization for $x=0.4$ when the magnetic field is applied along the *a* axis. As shown in Fig. 7(a), the magnetization along the *a* axis (M_a) shows the metamagnetic transition around 5 T as clearly discerned in the field-derivative curves (dM/dB). As shown in Fig. 7(c), this accompanies the polarization flop from P_a to P_c. Figure 7(d) shows the temperature dependence of magnetization (divided by the applied field strength) along the *a* axis at 0.01 and 5 T. As discussed above, a steep decrease in M_a at a low field at 24 K is due to the collinear to noncollinear magnetic transition accompanying the onset of P_a. On the other side, M_a at 5 T show no appreciable thermal variation down to the lowest temperature nor even upon the ferroelectric phase transition (26 K) with the onset of P_c [Fig. 7(f)]. In the FE-P_c phase, the magnetic structure should differ from the *ab*-plane cycloidal structure of the Mn spins anticipated for in the FE-P_a phase. The magnetic and temperature dependence of the wave number (q_l) and the intensity of superlattice peak are shown in Figs. 7(b) and 7(e), respectively. The superlattice peak shows no change in q_l upon the polarization flop though slightly decreasing its intensity. In the case of $TbMnO_3$, by the contrast, it shows the dramatic change of q_l from incommensurate phase ($q_l \sim 0.56$) to commensurate phase ($q_l = 0.5$) upon the polarization flop from P_c to P_a with a magnetic field along the *b* axis (H_b).[22] All the results suggest that the P_a and P_c phase in $Eu_{0.6}Y_{0.4}MnO_3$ arise from the incommensurate cycloidal spin structure where the spiral spin basal plane lie in the *ab* and *bc* plane, respectively. Recently, the same phenomenon the polarization flop transition without incommensurate-to-commensurate change of wave vector was reported for $DyMnO_3$.[26] The authors argued that the phenomenon may be responsible for the giant magnetocapacitance effect observed in $DyMnO_3$ close to tricritical point. In fact, $Eu_{0.6}Y_{0.4}MnO_3$ also show a similar giant magnetocapacitance effect $\Delta\epsilon_a/\epsilon_a(0\ \mathrm{T}) \sim 0.5$ (e.g., ~ 0.1 for $TbMnO_3$) at the polarization flop transition [Fig. 7(c)],[3] although the magnitude is smaller than the case of $DyMnO_3$ [e.g., $\Delta\epsilon_a/\epsilon_a(0\ \mathrm{T}) \sim 5$].[4] For understanding the giant magnetocapacitance in these compounds with the polarization flop, the dynamics of the domain walls between the P_a- and P_c-phase regime has to be clarified.

Both $TbMnO_3$ and $Eu_{0.6}Y_{0.4}MnO_3$ commonly show the polarization flop by applying a magnetic field, but the directions of ferroelectric polarization and driving magnetic field are different. In addition, the change in q_l upon the phase transition is also different although q_l in zero magnetic fields is very close (Table I). As for such a magnetic field effect on the ferroelectricity of spiral magnetic origin, the rotation of ferroelectric polarization is likely to be induced by the rotation of the spiral spin basal plane. In the case of $TbMnO_3$, however, the rotation of the basal plane from *bc* (P_c) to *ab* (P_a) by magnetic field H_b, can hardly be reconciled without consideration of the Tb $4f$-moment action. There would also

TABLE I. Comparison of the change of ferroelectric polarization and wave number of lattice modulation (q_l) upon the magnetic field induced ferroelectric phase transitions for $TbMnO_3$ and $Eu_{0.6}Y_{0.4}MnO_3$. The column of H indicates the magnetic field direction where the ferroelectric phase transition is induced. In $TbMnO_3$, the $H \| a$ can also induce the $P_c \rightarrow P_a$ flop but at high field (~ 10 T)[5].

	H	Polarization	Wave number q_l
$TbMnO_3$	$H \| b$	$P_c \rightarrow P_a$	0.56(IC) $\rightarrow$ 0.5(C)
$Eu_{0.6}Y_{0.4}MnO_3$	$H \| a$	$P_a \rightarrow P_c$	0.58(IC) $\rightarrow$ 0.58(IC)

be a possibility of the commensurate collinear spin structure which potentially hosts P_a. On the other hand, in the case of $Eu_{0.6}Y_{0.4}MnO_3$, it is reasonable to assign the mechanism to the rotation of the basal plane from ab (P_a) to bc (P_c) by magnetic field H_a, as in the case of spin flop transition in a conventional antiferromagnet. In weak fields the spins rotate in the ab plane with the ferroelectric polarization along the a axis (P_a), whereas in a strong magnetic field the spins tend to form a cone spiral with the uniform magnetization along the a axis that will force the spin spiral plane to lie in the bc plane with polarization P_c.

IV. CONCLUSION

In summary, we have presented a systematic study of magnetic-field effects on the magnetic, lattice-structural, and dielectric properties for single crystals of $Eu_{1-x}Y_xMnO_3$ ($0 \leqslant x \leqslant 0.4$) with orthorhombically distorted perovskite structure without $4f$ moment of rare earth ions. The weakly ferromagnetic phase (WFM) with the magnetization along the c axis is present in lower-x region ($x \leqslant 0.2$), whereas the ferroelectric phase (FE-P_a) occurs for $x=0.3$. For $x=0.4$, the successive ferroelectric transitions with the component of P_c and then P_a occur with lowering temperature even in the absence of magnetic field. Emergence of anisotropy in magnetization upon the ferroelectric transition indicates that Mn $3d$ spins undergo the collinear to noncollinear transition with the spiral ab plane for the FE-P_a phase in $x=0.3$ and 0.4. By investigation of synchrotron x-ray diffraction, we have observed no change in the wave number upon the ferroelectric transition, neither in the commensurate wave number $q_l = 0.5$ for $x=0.3$, nor in the incommensurate wave number $q_l \sim 0.58$ for $x=0.4$. Therefore, the ferroelectric polarization for $x=0.4$ (and likely for $x=0.3$) should be induced by the Mn $3d$ spin collinear to noncollinear transition rather than the collinear-incommensurate to collinear-commensurate one for $Eu_{1-x}Y_xMnO_3$. When a magnetic field is applied along the a axis for $Eu_{1-x}Y_xMnO_3$ ($x=0.4$), the direction of electric polarization is changed from P_a to P_c, that is the inverse direction to the case of $TbMnO_3$ and $DyMnO_3$. This polarization flop accompanies little change in the magnetic susceptibility nor in the lattice modulation wave number. Therefore, it is concluded that the thermally and magnetic-field induced polarization flop is induced by the rotation of the Mn $3d$ spins basal plane between the ab plane (P_a) and the bc plane (P_c), rather than the change of lattice modulation wave number q_l. All the magnetic field induced changes for $Eu_{1-x}Y_xMnO_3$ can be reasonably accounted for in terms of the spin-flop-like transition of the cycloidal spin structure: The difference in magnetic anisotropy with respect to the a and c axis are inherently weak as compared with that to the b axis, and hence the ab and bc plane cycloidal structures appear to be nearly degenerate. Conversely, the present work highlights the important role of the correlation between $4f$ moments and Mn $3d$ spins in the magnetic-field induced ferroelectric phase transitions of $TbMnO_3$ and $DyMnO_3$.

ACKNOWLEDGMENTS

The authors thank H. Sawa for his help in synchrotron x-ray measurements. This work was supported in part by Grant-In-Aids for Scientific Research (Grants No. 15104006, No. 17340104, No. 16076205, and No. 16076207) from the MEXT of Japan.

*Present address: Department of Physics, Osaka University, Osaka 560-0043, Japan.

[1] See, for example, M. Fiebig, J. Phys. D **38**, R123 (2005).
[2] Y. Tokura, Science **312**, 1481 (2006).
[3] T. Kimura, T. Goto, H. Shintani, K. Ishizaka, T. Arima, and Y. Tokura, Nature (London) **426**, 55 (2003).
[4] T. Goto, T. Kimura, G. Lawes, A. P. Ramirez, and Y. Tokura, Phys. Rev. Lett. **92**, 257201 (2004).
[5] T. Kimura, G. Lawes, T. Goto, Y. Tokura, and A. P. Ramirez, Phys. Rev. B **71**, 224425 (2005).
[6] M. Kenzelmann, A. B. Harris, S. Jonas, C. Broholm, J. Schefer, S. B. Kim, C. L. Zhang, S.-W. Cheong, O. P. Vajk, and J. W. Lynn, Phys. Rev. Lett. **95**, 087206 (2005).
[7] T. Arima, A. Tokunaga, T. Goto, H. Kimura, Y. Noda, and Y. Tokura, Phys. Rev. Lett. **96**, 097202 (2006).
[8] Y. Yamasaki, H. Sagayama, T. Goto, M. Matsuura, K. Hirota, T. Arima, and Y. Tokura, Phys. Rev. Lett. **98**, 147204 (2007).
[9] M. Mostovoy, Phys. Rev. Lett. **96**, 067601 (2006).
[10] I. A. Sergienko and E. Dagotto, Phys. Rev. B **73**, 094434 (2006).
[11] H. Katsura, N. Nagaosa, and A. V. Balatsky, Phys. Rev. Lett. **95**, 057205 (2005).
[12] G. Lawes, A. B. Harris, T. Kimura, N. Rogado, R. J. Cava, A. Aharony, O. Entin-Wohlman, T. Yildrim, M. Kenzelmann, C. Broholm, and A. P. Ramirez, Phys. Rev. Lett. **95**, 087205 (2005).
[13] K. Taniguchi, N. Abe, T. Takenobu, Y. Iwasa, and T. Arima, Phys. Rev. Lett. **97**, 097203 (2006).
[14] S. Park, Y. J. Choi, C. L. Zhang, and S.-W. Cheong, Phys. Rev. Lett. **98**, 057601 (2007).
[15] Y. Yamasaki, S. Miyasaka, Y. Kaneko, J.-P. He, T. Arima, and Y. Tokura, Phys. Rev. Lett. **96**, 207204 (2006).
[16] T. Arima, T. Goto, Y. Yamasaki, S. Miyasaka, K. Ishii, M.

Tsubota, T. Inami, Y. Murakami, and Y. Tokura, Phys. Rev. B **72**, 100102(R) (2005).

[17] N. Aliouane, D. N. Argyriou, J. Strempfer, I. Zegkinoglou, S. Landsgesell, and M. v. Zimmermann, Phys. Rev. B **73**, 020102(R) (2006).

[18] K. Noda, M. Akai, T. Kikuchi, D. Akahoshi, and H. Kuwahara, J. Appl. Phys. **99**, 08S905 (2006).

[19] J. Hemberger, F. Schrettle, A. Pimenov, P. Lunkenheimer, V. Y. Ivanov, A. A. Mukhin, A. M. Balbashov, and A. Loidl, Phys. Rev. B **75**, 035118 (2007).

[20] For $x=0.2$ in $Eu_{1-x}Y_xMnO_3$, a magnetic phase (AFM-3), which is weakly ferromagnetic and conelike magnetic structure, was reported in Ref. 19. However, we did not observe such a magnetic phase in our measurements of electric polarization and synchrotoron x-ray diffraction. The discrepancy of the reported results may be explained in terms of the nonstoichiometry of the samples (Ref. 21).

[21] T. Goto, Y. Yamasaki, H. Watanabe, T. Kimura, and Y. Tokura, Phys. Rev. B **72**, 220403(R) (2005).

[22] Dzyaloshinskii, J. Phys. Chem. Solids **4**, 241 (1958).

[23] T. Moriya, Phys. Rev. **120**, 91 (1960).

[24] T. Kimura, S. Ishihara, H. Shintani, T. Arima, K. T. Takahashi, K. Ishizaka, and Y. Tokura, Phys. Rev. B **68**, 060403(R) (2003).

[25] T. Kimura, JPSJ Online-News and Comments (Nov. 10, 2006).

[26] J. Strempfer, B. Bohnenbuck, M. Mostovoy, N. Aliouane, D. N. Argyriou, F. Schrettle, J. Hemberger, A. Krimmel, and M. v. Zimmermann, Phys. Rev. B **75**, 212402 (2007).